Anaerobic pyrite oxidation rates determined via direct volume-loss measurements: a Vertical Scanning Interferometric approach

E. R. Avery* and L. G. Benning

Earth and Biosphere Institute, School of Earth and Environment, University of Leeds, Leeds LS2 9JT, UK

ABSTRACT

Presented here are quantitative dissolution rate data (volume of pyrite lost/time) for the inorganic oxidation of pyrite in synthetic, anaerobic and acidic (pH 2) hydrothermal vent fluids (HVF) from experiments where the volume loss was measured directly via Vertical Scanning Interferometry (VSI). The VSI-derived reaction rate was $2.12 \times 10^{-10} \pm 1.14 \times 10^{-11}$ mol/m^2/min, which is ~2 to 4 orders of magnitude slower than pyrite oxidation rates previously determined using traditional batch experiments where rates are calculated based on changes in solution chemistry. This lower rate stems primarily from differences in experimental conditions (i.e. water to rock ratios, vigorous *vs.* gentle stir rates, grain-size effects, time), yet the rates derived here are believed to be more representative of pyrite oxidation in natural environments where more static and high solution to solid rate conditions prevail, such as seafloor conditions or acid-mine-drainage environments.

Introduction

SULPHIDE oxidation and weathering are important processes that govern the global Fe and S cycles both in terrestrial habitats, where sulphide oxidation gives rise to acid rock drainage (ARD), and at deep sea hydrothermal vents, where sulphide oxidation provides the necessary energy source to a large variety of biological processes. There have been many field-based studies investigating the ARD-related inorganic and biogenic mechanisms of sulphide oxidation (e.g. Smith and Schumate, 1970; McKibben and Barnes, 1986; Williamson and Rimstidt, 1994; Schippers, 2004) and recently some studies also followed the inorganic and biological pyrite oxidation processes in deep-sea environments (see Edwards *et al.* 2003, and references therein). However, most laboratory studies typically used the changes in bulk solution chemistry (normally [Fe$_{aq}$] and pH), normalized to the surface area (SA) of the pyrite in

equilibrium with the solution to derive rates. Although some studies have used BET analyses to determine pre- and post-reaction changes in the SA of pyrite, overall the rates reported in the literature (see Table 1) were based on pre-experiment determined SA and the changes in Fe^{2+}/Fe^{3+} and pH during the reaction (e.g. equation 1, Williamson and Rimstidt, 1994).

$$r = 10^{-8.58(\pm 0.15)} \times \frac{m_{Fe^{3+}}^{0.30(\pm 0.02)}}{m_{Fe^{2+}}^{0.47(\pm 0.03)} m_{H^+}^{0.032(\pm 0.04)}} \quad (1)$$

Recently atomic force microscopic (AFM) and vertical scanning interferometric (VSI) studies have shown that high-resolution surface measurements can provide very precise information about dissolution reactions based on changes of the surface characteristics of various minerals (e.g. Beig and Lüttge 2006; Lüttge *et al.* 1999; Arvidson *et al.* 2004). However, unlike AFM, VSI can provide height-resolution surface images of much larger areas with no loss in vertical accuracy and this allows a more robust determination of dissolution/precipitation kinetic rates. A VSI assessment of pyrite dissolution rates by VSI

has been published recently (Asta *et al.*, 2008) with applications to oxic ARD processes.

Presented here are rate data for the inorganic oxidation of pyrite in synthetic anaerobic hydrothermal vent fluids. Experiments where the direct and quantitative measurement of the 3D volume of pyrite lost over the course of the reactions (mol/m^2/min) from pre- and post-reacted samples were evaluated by VSI. The volumes obtained were used to derive a VSI-based rate, which was in turn compared and contrasted where the rate determined from VSI-type experiments was derived from the changes in solution composition (CHEM rates).

Methods and materials

Triplicate experiments using single, non-cleaved and cleaned pyrite grains (~1.5 mm^3) were conducted for periods between 18 and 93 days. A 3D topographic VSI surface map of each grain was obtained prior to masking ¼ of the grain surface with silicon glue (in order to preserve a reference area). After each experiment, the mask was removed, the sample was cleaned, and a second VSI scan obtained. Each 3D topographic image was converted to a 3D matrix and, using the *Surfer* software package (Golden Software, Inc., 1997), a 3D volume-loss for each individual grain was calculated from the difference between the pre- and post-reaction matrices. Thus, a direct and quantitative 3D volume loss which was then converted to mass lost (expressed as moles of pyrite/surface area (m^2)) was obtained. The errors in this approach were validated by analysing the

same surface at various scales (50 μm × 50 μm, 200 μm × 200 μm, 600 μm × 600 μm). In the batch experiments the bulk chemical changes in the solution composition (e.g. Fe^{2+}/Fe^{3+}) were used to determine the bulk chemical rate (CHEM).

Results and discussion

A typical VSI scan acquired after the reaction (Fig. 1) shows various dissolution/pitting features on the surface. Also clearly visible is the well preserved reference surface (masked during reaction) that was used to correlate the pre- and post-reaction data matrices.

From all experiments the lost mass expressed as moles of pyrite/surface area (m^2) was derived (Fig. 2) and a reaction rate of $2.12 \times 10^{-10} \pm 1.14 \times 10^{-11}$ mol/m^2/min was obtained. In Table 1 this rate is compared with the CHEM-derived rates as well as with rates obtained from the literature (recalculated using equation 1). The data show that the rate calculated from the direct VSI evaluations of mass loss in this study was 2 to 4 orders of magnitude less than previously published data. Possible contributing factors may be: (1) relatively static *vs.* dynamic conditions (gentle *vs.* rapid stir rates; no grain abrasion in the present study); (2) different water to rock ratio (0.05 *vs.* 0.94); (3) temperature (27ºC *vs.* 37ºC); (4) grain-size effects (single natural surface *vs.* 2−3 g of 180−250 μm-sized crushed pyrite). Chemical data collected during VSI-type experiments (CHEM) that were run in tandem with the VSI dissolution data yielded rates comparable to the rates
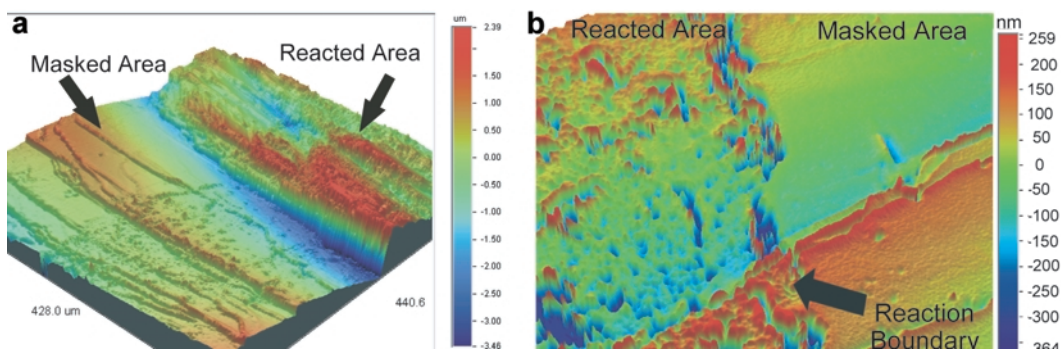

FIG. 1. 3D VSI image of a natural pyrite surface reacted with synthetic hydrothermal vent fluid at pH 2 for 67 days. (*a*) The dashed line is a guide to the eye to mark the interface between the cleaned but unreacted (formerly masked) surface and the pitted portion of the reacted sample. (*b*) Close up of the same region but at a higher resolution (40 μm × 40 μm) showing etch pits and substantial dissolution on the reacted surface
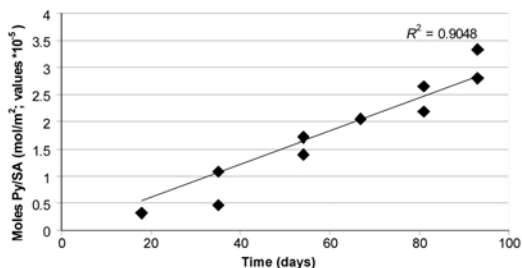
FIG. 2. Data were derived from the volume lost (using VSI); this was in turn converted to moles of pyrite using a pyrite density of 5 g/cm^3. The rate derived from this data is reported in Table 1 (VSI-derived).

determined using the direct VSI measurement of mass lost. Comparison with recently published VSI pyrite dissolution rates (Asta *et al.*, 2008) revealed the same close relationship between chemically derived rates and VSI-determined rates. However, the experiments conducted by Asta *et al.* (2008) were saturated with oxygen and were continuous flow experiments, two factors that contribute to the faster reaction rate. In addition, comparison of the VSI and chemically determined rates reported by Asta *et al.* (2008) with previous rates derived using batch experiments and aerobic conditions (McKibben and Barnes, 1986; Williamson and Rimstidt, 1994) yields rates that vary from each other by at least three orders of magnitude. Finally, it has to be

TABLE 1. Dissolution rates evaluated from direct VSI and chemical dissolution rate (CHEM) measurements in the present study compared with data from the literature for other oxygen-free pyrite-dissolution experiments. All data were recalculated using the rate law from Williamson and Rimstidt (1994, equation 1).

Data source	Rate (mol/m^2/min $\times 10^{-10}$)
This study, VSI	2.12
This study, CHEM	6.97
Williamson and Rimstidt (1994)	9600
McKibben and Barnes (1986)	86000
Smith and Shumate (1970)	4200
Asta *et al.* (2008), VSI*	1800
Asta *et al*. (2008), CHEM*	4320

* Under oxic conditions

noted that Asta *et al.* (2008) report orders of magnitude variations in the VSI derived oxidation rates and explain such large variations as due to the differences in surface reactivity. However, in the present study (1) the surface of the initial and post-reaction Py grains were cleaned carefully to remove adhered particles or possible newly precipitated material; (2) the natural Py surface was used; and (3) the changes in volume lost determined were evaluated at various scales (see methods) to determine the errors of this method. Our approach showed that overall the rates were up to three orders of magnitude less than previous batch experiments as well as the average rate reported by Asta *et al.* (2008).

Conclusions

Here, we present data from a study where the pyrite oxidation rate in hydrothermal-vent fluid-type systems was evaluated via direct measurement of volume loss from the surfaces of natural pyrite grains using VSI. These rates are more representative of pyrite oxidation in natural environments (e.g. seafloor or acid rock drainage conditions) where high solution to solid conditions and more static conditions usually prevail. The direct rates were two to four orders of magnitude slower than previous batch-experimental-derived rates. In addition, VSI provides a way to quantify dissolution rates in environments where *in situ* chemical monitoring is not feasible and the observed difference may indicate that batch dissolution rates of many mineral systems used in geochemical models may be vastly overestimated.

Acknowledgements

References

Arvidson, R.S., Beig, M.S. and Lüttge, A. (2004) Single-crystal plagioclase feldspar dissolution rates measured by vertical scanning interferometry. *American Mineralogist*, **89**, 51−56.

Asta, M.P., Cama, J., Soler, J.M., Arvidson, R.S. and Lüttge, A. (2008) Interferometric study of pyrite

surface reactivity in acidic conditions. *American Mineralogist*, **93**, 508−519.

Beig, M.S. and Lüttge, A. (2006) Albite dissolution kinetics as a function of distance from equilibrium: Implications for natural feldspar weathering. *Geochimica et Cosmochimica Acta*, **70**, 1402−1420.

Edwards, K.J., McCollom, T.M., Konishi, H. and Buseck, P.R. (2003) Seafloor bio-alteration of sulfide minerals: Results from *in-situ* incubation studies. *Geochimica et Cosmochimica Acta*, **67**, 2843−2856.

Golden Software, Inc. (1997) *Surfer (Win 32)* Ver. 6.04. Surface Mapping System.

Lüttge, A., Bolton, E.W. and Lasaga, A.C. (1999) An interferometric study of the dissolution kinetics of anorthite: the role of reactive surface area. *American Journal of Science*, **299**, 652−678.

McKibben, M.A. and Barnes, H.L. (1986) Oxidation of pyrite in low-temperature acidic solutions: rate laws and surface textures. *Geochemica et Cosmochimica Acta*. **50**, 1509−1520.

Schippers, A. (2004) Biogeochemistry of metal sulfide oxidation in mining environments, sediments, and soils. Pp. 83-96 in: *Sulfur Biogeochemistry − Past & Present* (J.A. Amend, K.J. Edwards, T. Lyons, editors). GSA publications, Geological Society of America, Boulder, Colorado.

Smith, E.E. and Shumate, K.S. (1970) *Sulfide to Sulfate Reaction Mechanisms*. Water pollution control series. 14010 FPS 02/70. USEPA, Washington, D.C.

Williamson, M.A. and Rimstidt, J.D. (1994) The kinetics and electrochemical rate-determining step of aqueous pyrite oxidation. *Geochemica et Cosmochimica Acta*, **58**, 5443−5454.